Appl Phys B (2010) 99: 695–700
DOI 10.1007/s00340-010-4030-x

Applied Physics B
Lasers and Optics

Antireflective properties of AZO subwavelength gratings patterned by holographic lithography

J.W. Leem · Y.M. Song · Y.T. Lee · J.S. Yu

Received: 12 October 2009 / Revised version: 4 April 2010 / Published online: 7 May 2010

Abstract We fabricate the aluminum-doped zinc oxide (AZO) subwavelength gratings (SWG) on Si and glass substrates by holographic lithography and sequent $CH_4/H_2/Ar$ reactive ion etching process. The etch selectivity of AZO over photoresist mask as well as the nano-scale shape is optimized for better antireflection performance. To analyze the antireflective properties of AZO SWG surface, the optical reflectivity is measured and then calculated together with a rigorous coupled-wave analysis. The reflectance spectrum can be considerably changed by incorporating the SWG into AZO film. As the SWG height of AZO on Si substrate increases, the magnitude of interference oscillations in the reflectance spectrum tends to be reduced with the larger difference between its maxima. The use of optimized SWG can significantly reduce the surface reflection of AZO film at the desired wavelengths. The measured reflectance data of AZO SWG are reasonably consistent with the simulation results. No considerable change in transmission characteristics is observed for AZO SWG structures.

1 Introduction

Antireflection layers have been often used to reduce the reflection of the surface in a certain wavelength range for optical components and optoelectronic devices [1, 2]. Single layer or multilayer thin films allow for antireflective properties due to the destructive interference of optical waves reflected from different interfaces [3]. However, the conventional technique has given rise to material selection issue, thermal expansion mismatch, and interfacial instability in the thin-film stacks [4, 5]. A subwavelength periodic structure with sizes smaller than the light wavelength can lead to the change in refractive index profile between the air to the semiconductor, providing a good thermal stability and durability [6, 7]. Recently, subwavelength gratings (SWG) have attracted considerable interest in optoelectronic device applications such as photovoltaic (PV) cells, photodetectors, and light emitting diodes because they can suppress farily the surface reflection over a wide wavelength range [8–13]. Although e-beam lithography or nano-imprint lithography has been usually employed to make the nano-sized patterns, holographic lithography is relatively simple, fast, inexpensive, and particularly applicable for large areas [11–13].

High-quality transparent conducting oxide (TCO) as window layer and top electrode layer is required for its use in optoelectronic devices. The aluminum-doped zinc oxide (AZO) film with a wide bandgap will be a promising alternative to indium tin oxide as TCO for PV applications because it has many advantages including high thermal stability, low cost, and non-toxicity [14, 15]. The AZO film with thickness above about 0.5 μm is often used because its resistivity is generally decreased with increasing the film thickness [16]. However, the incident light suffers from high reflection at specific wavelengths due to the high refractive index contrast between the AZO and semiconductor materials, thus degrading the device performance. Particularly, an effective light trapping is crucial in thin-film Si solar cells due to a low absorption coefficient. Although an additional antireflection layer, such as Al_2O_3, TiO_2 and Si_xN_y, has been mainly used, the SWG structure has the potential to min-

J.W. Leem · J.S. Yu (✉)
Department of Electronics and Radio Engineering, Kyung Hee University, 1 Seocheon-dong, Giheung-gu, Yongin-si, Gyeonggi-do 446-701, Republic of Korea
e-mail: jsyu@khu.ac.kr

Y.M. Song · Y.T. Lee
Department of Information and Communications, Gwangju Institute of Science and Technology, 1 Oryong-dong, Buk-gu, Gwangju 500-712, Republic of Korea

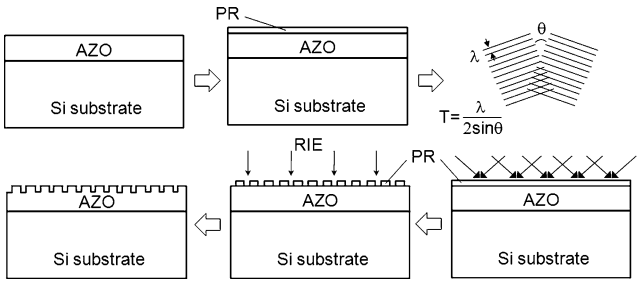

Fig. 1 Schematic diagram of the pattern transfer process steps for the fabrication of the SWG structures of AZO deposited on Si substrate

imize the reflection loss as mentioned above [17]. Furthermore, broadband and omnidirectional antireflection coatings are essential in covering a range of the solar spectrum for PV cells [18].

In this paper, we investigated the structural and optical properties of SWG structure of AZO deposited on Si and glass substrates by optimizing the process conditions using holographic lithography and dry etching in sequence to create the nano-structures. The optical reflectivity was theoretically analyzed by the rigorous coupled-wave analysis (RCWA) simulation.

2 Experimental details

The schematic diagram of the pattern transfer process steps for the fabrication of the SWG structures of AZO deposited on Si substrate is shown in Fig. 1. The AZO films were deposited on Si and glass substrates by using RF magnetron sputtering system at room temperature. The ZnO:Al (99.999% purity) target containing 2 wt% Al_2O_3 was used. The chamber was evacuated to a base pressure of $<1 \times 10^{-6}$ Torr. The process pressure was 5 mTorr in Ar environment and the RF sputtering power was 100 W. To obtain good uniformity, the substrate was rotated with 20 rpm during the sputtering. The samples were prepared with an AZO thickness of ∼600 nm. For the fabrication of SWG structures, AZ5206 photoresist (PR) was spin-coated on AZO/Si and AZO/glass substrates. The dilution ratio and rotation speed were adjusted to optimize the PR thickness. After prebaking on a hot plate at 90°C for 90 s, the coated PR was exposed twice by using a two-beam interference method with a 363.8 nm line of Ar ion laser to define two-dimensional periodic PR patterns. For a hexagonal pattern, the sample was rotated by 60° between exposures. After developing, the PR patterns were transferred onto AZO surfaces using a dry etching for SWG structures. The underlying AZO was etched by using $CH_4/H_2/Ar$ (1:2:1) reactive ion etching (RIE). The overall etching of PR patterned structure leads to extremely fast etching at the rim and slower etching at the center, producing a tapered profile grating. The etched profile and etch depth of the fabricated SWG structures were observed by using a scanning electron microscope (SEM). The specular reflectance and transmittance were measured by using a UV–VIS–NIR spectrophotometer.

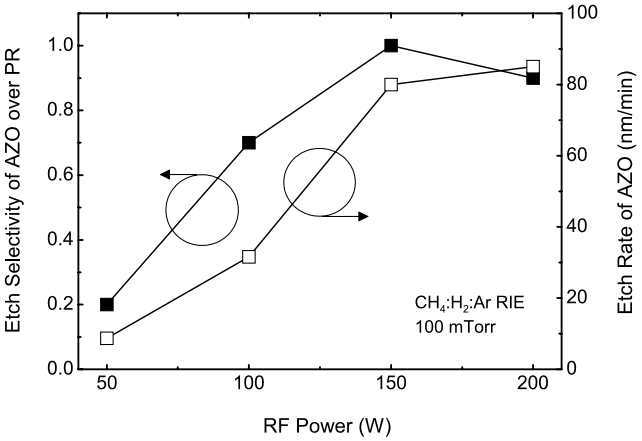

Fig. 2 Etch selectivity of AZO over PR and the etch rate of AZO for nano-sized patterns as a function of RF power in $CH_4/H_2/Ar$ plasma

3 Results and discussion

Antireflective characteristics strongly depend on the surface structure of AZO films. Thus, the etch selectivity and etch rate of AZO play an important role in achieving the efficient antireflection structure. Figure 2 shows the etch selectivity of AZO over PR and the etch rate of AZO for nano-sized patterns as a function of RF power in $CH_4/H_2/Ar$ plasma. The etch rate and etch selectivity were strongly dependant on the RF power. The etch selectivity of AZO to PR is very low (i.e., ∼0.2) at 50 W due to the low etch rate. The etch selectivity was increased with increasing RF power, but it was decreased at above 150 W. When the RF power is too high, it significantly enhances the erosion of PR mask pattern, leading to the reduction in etch selectivity. The etch selectivity of ∼1 was obtained at 150 W. The etch rate of AZO increased from 8.7 nm/min at 50 W to 85 nm/min at 200 W due to the increase in the number of active particles and in the ion energy flux as the RF power increased. Therefore, the etch depth can be controlled effectively by the PR thickness and etch selectivity.

Figure 3(a) shows the SEM images of the PR patterns (upper) and the etched SWG structures (lower) on AZO/Si substrates for the develop times of (i) 4 s, (ii) 6 s, and (iii) 8 s. The RF power of 150 W was chosen as an optimum as shown in Fig. 2 and the process pressure was 100 mTorr in $CH_4/H_2/Ar$ plasma. The PR thickness was about 150 nm and the etching time was set to 4 min at room temperature. The power of the Ar laser was fixed at 100 mW with an optimized exposure time of 21 s for the pattern period of 300 nm.

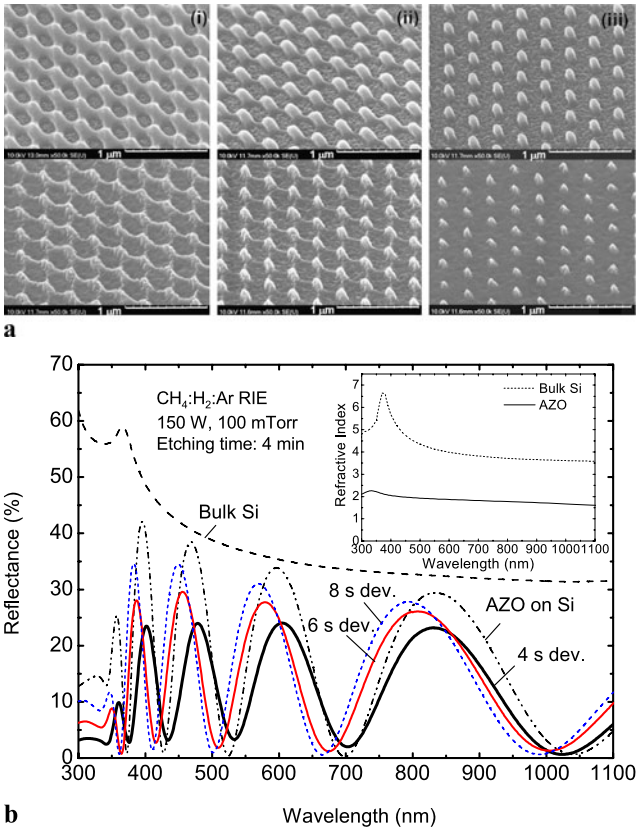

Fig. 3 (**a**) SEM images of the PR patterns (upper) and the etched SWG structures (lower) on AZO/Si substrates for the develop times of (i) 4 s, (ii) 6 s, and (iii) 8 s, and (**b**) measured reflectance spectra of the fabricated AZO SWG structures on Si substrate after 4 min $CH_4/H_2/Ar$ RIE for the develop times of 4 s, 6 s, and 8 s, together with bulk Si and AZO/Si. The *inset* of (**b**) shows the refractive index of bulk Si and AZO as a function of wavelength

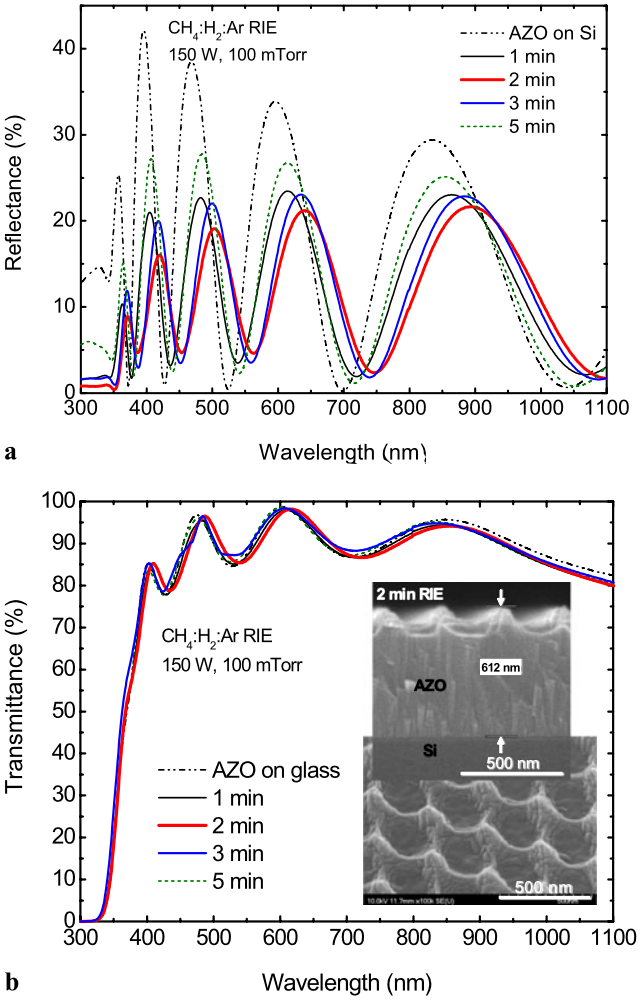

Fig. 4 (**a**) Measured reflectance of the fabricated AZO SWG on Si substrate and (**b**) measured transmittance of the fabricated AZO SWG on glass substrate as function of wavelength for the etching times of 1 min, 2 min, 3 min, and 5 min. The *inset* of (**b**) shows the SEM images of the fabricated AZO SWG structure with hole arrays after 2 min RIE. The PR develop time is optimized at 4 s

PR patterns can be changed by develop time as shown in Fig. 3(a). As the develop time of PR increased, the open hole became broaden because the PR was over-developed. For 8 s develop time, the dot patterns were formed. The PR patterns were used as an etch mask to transfer patterns into AZO films through sequential RIE. The etching was performed until the mask was completely removed. The etched patterns were replica of the PR patterns with a serious undercut. The serious undercuts are attributed to the excessive overetching.

Figure 3(b) shows the measured reflectance spectra of the fabricated AZO SWG structures on Si substrate after 4 min $CH_4/H_2/Ar$ RIE for the develop times of 4 s, 6 s, and 8 s. For comparison, the reflectance of bulk Si and AZO/Si is also shown. The inset shows the refractive index of bulk Si and AZO as a function of wavelength. For bulk Si substrate, the reflectance was high, i.e., more than 32% at wavelengths of 300–1100 nm. Strong oscillations were observed clearly below the band edge in reflectance spectra of AZO/Si due to the constructive or destructive interference of light at different wavelengths by multiple internal reflections between the AZO surface and AZO/Si interface, indicating the reflectance maxima of >30%. As expected, the reflectance was not much reduced for the dot arrays because the density of dots is low with small size. The undesirable undercut may be caused inherently during the RIE by the PR patterns on the rough surface of AZO deposited by the sputtering method. Thus, it is difficult to obtain the closely packed dot arrays due to the undercut effects. In contrast, for the hole arrays fabricated after 4 s developing, the maximum values of reflectance were reduced to <25%. It is clear that the average reflectivity of the AZO SWG with hole arrays in the visible wavelength range is reduced compared to the conventional AZO film.

Figure 4(a) shows the measured reflectance of the fabricated AZO SWG on Si substrate as function of wavelength for the etching times of 1 min, 2 min, 3 min, and 5 min.

Table 1 Develop time, etching time, PR thickness, AZO thickness, hole/pillar diameter, pitch, and etch depth for the fabricated AZO structures

Develop time (s)	Etching time (min)	Photoresist thickness (nm)	AZO thickness (nm)	Hole/pillar diameter (nm)	Pitch (nm)	Etch depth (nm)
4	4	150	600	$184 \pm 10/124 \pm 12$	116 ± 5	101 ± 4
6	4	140	600	$202 \pm 10/106 \pm 10$	100 ± 5	87 ± 4
8	4	120	600	$-/83 \pm 10$	80 ± 3	70 ± 3
4	1	150	600	$162 \pm 8/142 \pm 6$	105 ± 4	83 ± 3
4	2	150	600	$174 \pm 8/138 \pm 8$	162 ± 5	150 ± 4
4	3	150	600	$179 \pm 10/125 \pm 10$	134 ± 4	122 ± 4
4	5	150	600	$189 \pm 12/116 \pm 10$	96 ± 3	73 ± 3
4	3	220	600	$143 \pm 8/159 \pm 12$	232 ± 10	224 ± 5

The PR develop time was optimized at 4 s. The reflectance of AZO SWG structures was reduced as the etching time increased up to 2 min. For longer etching than 2 min, the reflectance was increased with etching time. After 5 min of etching, the sample exhibited clearly higher maximum values compared to the etched one for 4 min as shown in Fig. 3(b). This is attributed mainly to the deformation of SWG structures caused by overetching. From the SEM observations, the 2 min is enough to completely remove the PR patterns during the overall etching, leading to a SWG height of ~150 nm. With a further etching, the SWG height of AZO became lower due to the overetching. It is noted that the slight shift of reflectance maxima of AZO SWG structures with respect to AZO film is probably due to the variations of film thickness. The inset of Fig. 4(b) shows the SEM images of the fabricated AZO SWG structure with hole arrays on Si substrate after 2 min RIE. The AZO SWG with hole arrays, which are approximately tapered cross-sectional shapes, have larger height compared to one as shown in Fig. 3(a) though it still has a slight undercut. For the shorter wavelength region, the decrease in the reflectance of SWG structures was enhanced. For the etching time of 2 min, the optimized SWG structure was obtained, indicating a relatively low reflectance over a wide wavelength range. Around a wavelength of 400 nm, the maximum of reflectance was dramatically reduced from 42.1% to 16%. The develop time, etching time, PR thickness, AZO thickness, hole/pillar diameter, pitch, and etch depth for the fabricated AZO structures are summarized in Table 1.

For transmittance measurements, the AZO films were also deposited on glass substrate. The measured transmittance spectra of the fabricated AZO SWG on glass substrate are shown in Fig. 4(b). For conventional AZO film, it shows a typical transmission spectrum with the interference feature. The average transmittance of >90% with an absorption edge at ~340 nm was obtained in the visible wavelength range, indicating overall good quality of AZO film with high transparency. There is no shift of the absorption edge for AZO SWG structures. The similar transmittance for the AZO film on glass and the structured AZO indicates that the scattering in the structured films is not relevant. The transparent characteristics were not noticeably affected by the introduction of SWGs into the AZO surface.

For theoretical analysis, the reflectance calculations of AZO SWG structures on Si were carried out by using the RCWA method [19]. The AZO can be considered to be only intrinsic because the effect of impurity doping on the optical properties is negligible. In the calculations, the model was constructed approximately to three-dimensional AZO tapered pillars with 6-fold hexagonal symmetry structure on Si substrate. The 5th order of diffraction was used to calculate the diffraction efficiency, which is a sufficient number to stabilize the results numerically. The dispersion of Si and AZO was also considered to obtain the exact result at each wavelength. In the contour plot, the resolution of height and wavelength was set to 10 nm. The structural geometry of the tapered pillars for the calculations was shown in previous reports [10, 20]. Figure 5(a) shows the measured and calculated reflectance spectra of the fabricated AZO SWG structures on Si substrate using 150 nm and 220 nm thick PRs. The inset shows the SEM images of 220 nm thick PR patterns and AZO SWG structure with hole arrays after 3 min RIE. After longer etching using 220 nm thick PR, the height of AZO SWG was increased. For the larger height of AZO SWG, the distance between the reflectance maxima became longer, indicating a reduction of film thickness. The reflectance was relatively decreased for 220 nm thick PR and its maxima were less than 16% (21% for 150 nm thick PR) in the wavelength range of 300–800 nm. However, the values of reflectance at the minima were also increased. Although there is a discrepancy between the measured and calculated results at wavelengths of 350–550 nm for the sample with a 3 min etching time because it is difficult to exactly match the geometric simulation model to the actual fabricated structure, the overall trends are similar for relatively different SWG heights. Clearly, the magnitude of interference oscillations in reflectance spectrum was decreased and the distance between its maxima was increased for the larger

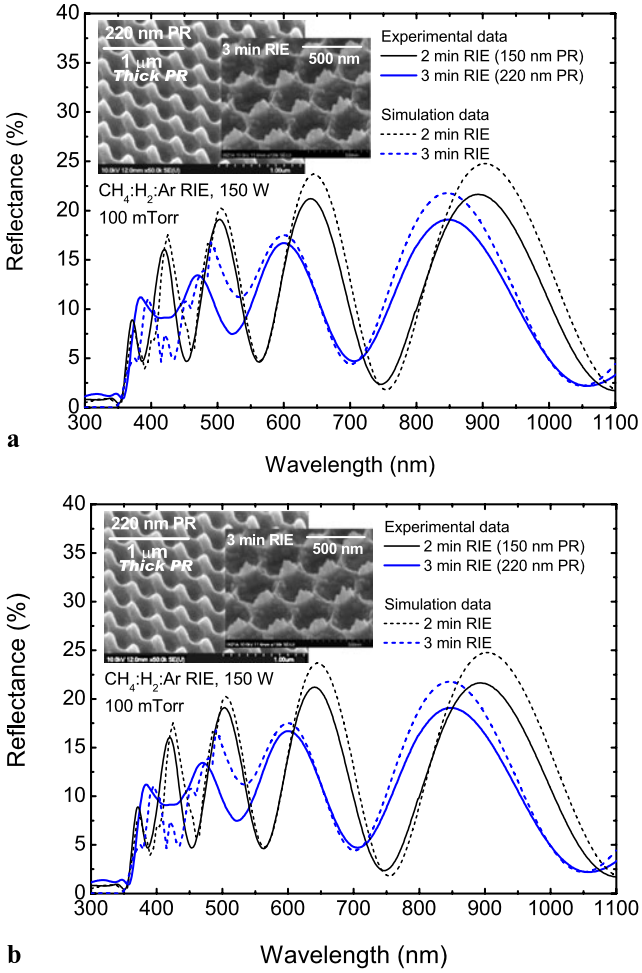

Fig. 5 (**a**) Measured and calculated reflectance spectra of the fabricated AZO SWG structures on Si substrate using 150 nm and 220 nm thick PRs, and (**b**) calculated reflectance spectra of AZO SWG structures with 300 nm and 400 nm heights on Si substrate. The *inset* of (**a**) shows the SEM images of 220 nm thick PR patterns and AZO SWG structure with hole arrays after 3 min RIE

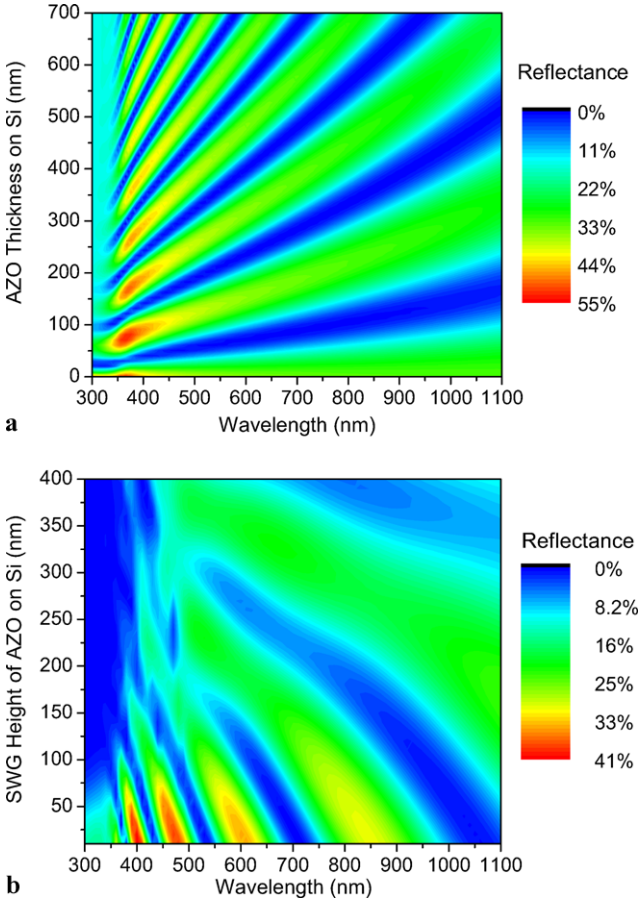

Fig. 6 (**a**) Contour plot of the variation of reflectance spectra as a function of AZO thickness on Si substrate and (**b**) contour plot of the variation of reflectance spectra as a function of SWG height of AZO on Si substrate for a SWG period of 300 nm. In (**b**), the AZO thickness is fixed at 600 nm

SWG height from simulation results in Fig. 5(b). However, the reflectance minima are also increased noticeably when the height is too large.

A number of simulations give a deep insight into the optical reflectivity of the AZO SWG structure on Si substrate. Figure 6(a) shows the contour plot of the variation of reflectance spectra as a function of AZO thickness on Si substrate. The interference oscillations in the reflectance increase as the thickness of AZO on Si substrate increases. For the AZO thickness of 100 nm, the low reflectance of $<10\%$ was obtained in the wavelength region of 600–1100 nm, but it exhibited a high reflectance without low reflectance bands at shorter wavelengths. The low reflectance band was split and it got narrower with the increase of AZO thickness. For the AZO thickness of 700 nm, it increased the number of minima close to 0% and maxima of $>30\%$. As the wavelength increased, the low reflection band became broaden.

The contour plot of the variation of reflectance spectra as a function of SWG height of AZO on Si substrate for a SWG period of 300 nm is shown in Fig. 6(b). The AZO thickness was fixed at 600 nm. The use of SWG structure significantly changed the reflectance spectra. The interference oscillations were reduced with the larger distance between the maxima in reflectance spectra as the SWG height of AZO increased. At the SWG height of 150 nm, the maxima were considerably decreased. However, for larger SWG heights, the minima also increased to the reflectance value of $>10\%$. Therefore, the SWG height of AZO on Si substrate should be properly chosen to achieve the low reflectance over a wide wavelength region.

4 Conclusion

To reduce the surface reflection of AZO film, the AZO SWG structures on Si substrate fabricated by holographic lithography and dry etching were investigated, together with theoretical analysis using RCWA simulation. The $CH_4/H_2/Ar$

RIE with high etch selectivity of AZO over PR was used for the fabrication of AZO SWG structures. The surface reflection of AZO film was substantially decreased by the optimized SWG structure over a wide wavelength range. It is found that the interference oscillations in reflectance spectrum were reduced with increasing the SWG height, but its minima were substantially increased for a too large height. Also the distance between the maxima in reflectance spectra became larger. The measured results of the fabricated AZO SWG structures were reasonably consistent with the simulated results, indicating no considerable change in transmission characteristics. From simulation results, the geometric SWG structure should be optimized for a low surface reflection at the required wavelengths for use in various applications.

Acknowledgements The work was supported by the Korea Science and Engineering Foundation (KOSEF) grant funded by the Ministry of Education, Science and Technology (MEST) (No. 2009-0070459 and 2009-0077580).

References

1. B.B. Shi, Z.Q. Ma, X. Tang, C.B. Feng, Proc. SPIE **6984**, 69843D (2008)
2. M.F. Schubert, F.W. Mont, S. Chhajed, D.J. Poxson, J.K. Kim, E.F. Schubert, Opt. Express **16**, 5290 (2008)
3. J. Zhao, M.A. Green, IEEE Trans. Electron Dev. **38**, 1925 (1991)
4. P. Lalanne, G.M. Morris, Proc. SPIE **2776**, 300 (1996)
5. S. Walheim, E. Schaffer, J. Mlynek, U. Steiner, Science **283**, 520 (1999)
6. S.J. Wilson, M.C. Hutley, Opt. Acta **29**, 993 (1982)
7. S.A. Boden, D.M. Bagnall, Appl. Phys. Lett. **93**, 133108 (2008)
8. H. Sai, H. Fujii, K. Arafune, Y. Ohshita, Y. Kanamori, H. Yugami, M. Yamaguchi, Jpn. J. Appl. Phys. **46**, 3333 (2007)
9. H.K. Kanamori, H. Sai, H. Yugami, Appl. Phys. Lett. **78**, 142 (2001)
10. Y.M. Song, S.Y. Bae, J.S. Yu, Y.T. Lee, Opt. Lett. **34**, 1702 (2009)
11. K. Wensu, S.C. Huang, A. Kechiantz, C.P. Lee, Opt. Quantum Electron. **37**, 425 (2005)
12. Z. Yu, H. Gao, W. Wu, H. Ge, S.Y. Chou, J. Vac. Sci. Technol. B **21**, 2874 (2003)
13. K. Kintaka, J. Nishii, A. Mizutani, H. Kikuta, H. Nakano, Opt. Lett. **26**, 1642 (2001)
14. I. Stambolova, K. Konstantinov, S. Vassilev, P. Peshev, T.S. Tsacheva, Mater. Chem. Phys. **63**, 104 (2000)
15. Z.B. Ayadi, L.E. Mir, K. Djessas, S. Alaya, Nanotechnology **18**, 445702 (2007)
16. B.Z. Dong, G.J. Fang, J.F. Wang, W.J. Guan, X.Z. Zhao, J. Appl. Phys. **101**, 033713 (2007)
17. F. Chaabouni, M. Abaab, B. Rezig, Superlattices Microstruct. **39**, 171 (2006)
18. S.L. Diedenhofen, G. Vecchi, R.E. Algra, A. Hartsuiker, O.L. Muskens, G. Immink, E.P.A.M. Bakkers, W.L. Vos, J.G. Rivas, Adv. Mater. **21**, 973 (2009)
19. M.G. Moharam, Proc. SPIE **883**, 8 (1988)
20. Y.M. Song, J.S. Yu, Y.T. Lee, Opt. Lett. **35**, 276 (2010)